Ecological Modelling 221 (2010) 1378–1393

Contents lists available at ScienceDirect

Ecological Modelling

journal homepage: www.elsevier.com/locate/ecolmodel

Effects of temperature variation on TSD in turtle (*C. picta*) populations

Amy Parrott [a,*], J. David Logan [b]

[a] Department of Mathematics, University of Wisconsin Oshkosh, 800 Algoma Blvd, Oshkosh, WI 54901, United States
[b] Department of Mathematics, University of Nebraska Lincoln, United States

ARTICLE INFO

Article history:
Received 2 October 2009
Received in revised form 1 February 2010
Accepted 12 February 2010
Available online 20 March 2010

Keywords:
Temperature dependent sex determination (TSD)
Turtle ecology
Global temperature change
Two-sex model

ABSTRACT

We formulate a two-sex model of temperature-dependent sex determination (TSD) for a freshwater turtle (*C. picta*) population. The aim is to understand how environmental temperature variations and nest heat conduction properties affect the long term dynamics of the population. This is a key to understanding how global temperature changes may affect their survival. With stochastic inputs of ambient temperature and solar radiation, the model uses the heat equation to determine the temperature in the egg layer in the nest; in turn, this determines the sex ratio in the egg clutch using a variable degree-day model. Finally, a nonlinear Leslie type, stage-based, two-sex model, is used to determine the long term male and female populations. A two-sex model is required because of different development rates for males and females. The model is flexible enough to enable other researchers to examine the effects of temperature variation variations on other species with TSD, e.g., crocodilians, reptilians, as well as other turtle species. It can be adapted to study effects of nest location, soil type, rain events, different incubation periods, and density effects, for example, the dependence of the mating function on the ratio of males to females and each's contribution to the sex of hatchlings. Modifications can be easily made to fit a specific life history traits. The model is a beginning step in understanding the long term, high fitness shown by many reptile species with TSD, and it may suggest to experimentalists what data may be relevant to these issues; it can also be useful to wildlife managers in developing strategies for intervention if needed. Among the principal findings are that temperature variability and detailed nest heat conduction properties may buffer projected negative effects on a population.

1. Introduction

1.1. Temperature-dependent sex determination

Climate change and its effects on ecosystems is a major concern. The Intergovernmental Panel on Climate Change (IPCC), and others, report that warming of the planet is evident worldwide. They report the likelihood of increases in the frequency of heat waves as well as heat extremes (Bernstein et al., 2007). For certain species of animals, especially those that exhibit temperature-dependent sex determination (TSD), temperature variations pose a possibly serious threat. TSD is a evolutionary strategy in which the temperature during development of the organism determines the sex of the animal, in contrast to other organisms where sex is determined through chromosomes (Valenzuela and Lance, 2004). It is conceivable therefore, that if the temperature changes favor only one sex, then dire consequences for those populations and their ecosystems could occur. Survival of species exhibiting TSD may well depend on how well the species is suited to buffering the effects of the temperature change. TSD is seen in crocodilians, lizards, turtles, some fish, and even in some birds.

In this paper we examine effects that climate change, in particular, temperature variation, may have upon painted turtles (*Chrysemys picta*), a freshwater species with TSD. We investigate the magnitude and type of change required to have an adverse effect upon its population. Specifically, we look the effects caused by an increase in average temperature and a change in daily temperature variance on the nest. We develop a computational model that connects these environmental changes to the sex of the nests and subsequently to the male/female population structure. There seems to be no detailed model in the literature that incorporates variability of this type on populations and gender structure of species with TSD. There have been many studies performed in laboratory settings on the effects of temperature on sex (Bull et al., 1982; Chevalier et al., 1999; Demuth, 2001; Du and Ji, 2003; Janzen and Morjan, 2002; Shine and Harlow, 1996; Schwarzkpf and Brooks, 1985). The majority of these involve incubating the eggs at a constant temperature level. However, there have been very few studies on the influence of variable temperatures in actual nests (Bull, 1985; Georges, 1992; Janzen, 1994; Shine and Harlow, 1996). In summary, we show how to formulate a detailed, complete model of TSD with the following elements: stochastic temperature and

* Corresponding author. Tel.: +1 920 424 2305.
E-mail address: parrotta@uwosh.edu (A. Parrott).

0304-3800/$ – see front matter © 2010 Elsevier B.V. All rights reserved.
doi:10.1016/j.ecolmodel.2010.02.004

solar radiation inputs, a heat transfer model using the diffusion equation to obtain nest temperatures with different soil and egg layer conductivities, a degree-day model to determine the sex of the nest with a temperature-dependent incubation period, and a two-sex, stage-based population model that includes male and female contributions to egg numbers, female sperm storage, and a polyandrous female population.

In the study (Janzen, 1994), the average air temperature in July was correlated to the sex of the turtles, and then the result was extrapolated to determine that an increase of only 4 ° C could effectively eliminate the population. However, only the average monthly temperature was considered, and there was no account of the variability and the insulating effects that the air-soil mixture around the eggs. As part of our study, we model the temperature profile in a nest, given variable ambient air temperature and solar radiation, and we include the effects of heat conduction properties in the nest, specifically in the air and soil region in the egg layer. In contrast to (Janzen, 1994), we show that an increase of 4 ° C may not eliminate the population.

Woodward and Murray (1993) construct a model that describes dynamics for a population with TSD, assuming that the proportion of females each year is constant. In our model, both males and females, through a mating function weighted by yearly sperm storage properties, contribute to the egg production; stochastic temperature profiles inside the nest determines the proportion of females each year, calculated using a degree-hour approach. Georges (1989), Georges et al. (2005), and Valenzuela and Lance (2004) have developed a model for determining the sex of the nest based upon the temperature profile inside the nest, but the model is only valid for species with one temperature threshold. Because northern painted turtles have both upper and lower temperature thresholds, which is the case we examine, we modify their model to accommodate this change. Schwarzkopf and Brooks (1987) found that a degree-hour model best predicted the sex ratio of the nest.

As an aside, it is interesting to speculate why some species become extinct and others do not. Families of turtles, and other reptilians such as crocodilia, have survived and thrived millions of years with sometimes few changes. Of course, these species have a unique biology and social behavior that must contribute to their survival. But a crucial difference, as we noted, is that their sex is determined by temperature (TSD) during the egg incubation period, and not genetically like most other animals. Many have speculated how this trait has lent itself to the survival of turtles and other reptiles. Key to this question is: Why has TSD evolved? In turtles, where higher temperatures often favor female offspring, it has been speculated that higher temperatures favor the expression of the gene for the female-determining factor. Further, in a warm nest, eggs develop faster. For certain species this may mean that adult females are larger and can lay more eggs, and therefore have higher fitness. Others speculate that it is density dependence that governs the sex ratio rather than individual fitness. Temperature changes in the environment may lead to dynamics that favor one sex or the other in the birth function of a two-sex model. In different words, when the male population is low, there is an increase in contribution that males make to the birth function. In spite of these studies, the evolutionary benefit of TSD remains uncertain.

There are four widely held reasons for TSD persistence in reptiles, which are reviewed in Janzen and Phillips (2006) and Valenzuela and Lance (2004). First, fitness levels may be optimal for each sex at these temperatures (Warner and Shine, 2008). Although, Janzen and Phillips (2006) downplay the significance of this, stating that the research confirming this view conflicts with other research. Second, TSD allows the species to place some control over the sex ratio to promote group fitness (Schwarzkopf and Brooks, 1987). Third, TSD minimizes inbreeding by producing single-sex clutches (Janzen and Phillips, 2006). Fourth, there is no adaptive advantage to evolving away from TSD, so it is just maintained. See, for example, Murray (2002), for a brief, insightful discussion of TSD in crocodiles (the strategy being nest selection sites) and the associated literature. Information on TSD in freshwater turtles is far less extensive than crocodilia and other endangered sea turtles, e.g., loggerheads, perhaps because of extinction risks.

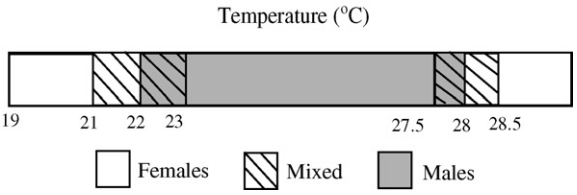

Fig. 1. Temperature thresholds of FMF type in western Nebraska populations of *C. picta*.

Although the model in this paper does not incorporate some of these evolutionary ideas, it can be adapted to address some of the issues involving natural selection and density dependence. Conducting numerical simulations under various scenarios in a model may lead to a better understanding of the roles of these influences. These are problems we point to for further study and analysis.

There are three major types of TSD: male–female (MF), where males are produced at cooler temperatures and females at warmer temperatures, female–male (FM), where females are produced at cooler temperatures and males at warmer temperatures, and female–male–female (FMF), where females are produced at both temperature extremes and males are produced in between. It is this latter case we examine for the *C. picta* population in Western Nebraska. While painted turtles in southern latitudes of the United States exhibit MF, Bull et al. (1982), Schwarzkpf and Brooks (1985), and Gutzke and Paukstis (1984) have shown that northern populations produce females at both cooler and warmer nest temperatures. The upper and lower thresholds show some variation among the populations. The upper threshold was found to be 27.5 ° C in Tennessee (Bull et al., 1982) and in Ontario (Schwarzkpf and Brooks, 1985), 28 ° C in Nebraska (Gutzke and Paukstis, 1984), and 28.5° C in Wisconsin (Bull et al., 1982). In Nebraska, the lower threshold was found to be 22 ° C (Gutzke and Paukstis, 1984), and in Ontario 20 ° C (Schwarzkpf and Brooks, 1985). It is speculated that the lower threshold is required because the ground temperature in northern climates seldom reaches a temperature above 28 ° C (Gutzke and Paukstis, 1984).

In this study, we use the threshold temperatures for the Nebraska turtles (see Fig. 1). The time of sex determination occurs during the middle third of the egg incubation period. We incorporate these facts in the model. If the majority of development during this time period occurs within the male temperature range, the nest will be male. If the majority of the development occurs within the female temperature range, the nest will produce females, and if the temperature oscillates about a threshold cutoff, the nest will produce both males and females (Valenzuela and Lance, 2004).

1.2. A brief on turtle ecology (C. picta)

In this section we summarize various observations of turtle ecology relevant to the development of our model. Key papers that present these data and contain more detail are Bartlett and Bartlett (2006), Cagle (1954), Ernst et al. (1994), Gibbons (1968), Iverson and Simith (1993), Rowe et al. (2003), Tinkle et al. (1981), Wilbur (1975a) and Wilbur (1975b).

C. picta is divided into four subspecies according to the region of North America it occupies. *C. picta picta* resides from southeastern Canada, down the coast to Georgia or Florida. *C. picta marginata* resides from southern Quebec and Ontario, south through Illinois

and then east through Tennessee, West Virginia, Virginia, and the Carolinas. *C. picta dorsalis* is found in southern Illinois and Missouri, down both sides of the Mississippi River to the Gulf of Mexico. *C. picta belli* resides from western Ontario to British Columbia, down through northern Oregon to Oklahoma. The habitat of *C. picta* consists primarily of slow moving waters such as lake coastlines, ponds, marshes, and creeks. The turtles generally begin their day around sunrise and are active for a period of time, after which they bask for several hours before foraging. Afterwards, they bask again until late afternoon or early evening when they again forage before spending the night sleeping in the water.

The differences between the subspecies are small, the main difference being the number and size of the clutches. There are several distinguishing features between the sexes. Mature males have longer fore claws and longer, thicker tails than those of females, and mature females are typically larger in overall size than males. A female can lay from one to five clutches per season, although two or three clutches are common. The number of eggs per clutch varies among subspecies. *C. picta bella* lays the most with 6–21 eggs, while *C. picta picta* lays 2–10 eggs and *C. picta marginata* lays 3–14 eggs. *C. picta dorsalis* lays the fewest number with 1–7 eggs on average per clutch. Our own experiments, where we X-rayed gravid females, confirm these numbers.

Painted turtles are opportunistic omnivores. Their diet consists of plant matter, algae, leaches, crayfish, spiders, mosquitoes, fish, frogs, and various other insects. Younger turtles tend to be mostly carnivorous while adults are primarily herbivores. Their activity level changes throughout the year. In northern climates the turtles become active in the early spring and remain active until ice begins again to form on the water. Then they hibernate under water, buried in the soft soil of the bottom or along the bank in burrows. In northern climates hibernation may last 5–7 months of the year, while in southern climates turtles may not hibernate at all.

Predators of painted turtles are dependent upon the size of the turtle. Hatchlings and juveniles are preyed upon by "rice rats, muskrats, mink, raccoons, snapping turtles, snakes, bullfrogs, large fish, heron, and water bugs." Adult turtles are often preyed upon by alligators, raccoons, bald eagles, osprey, red-shouldered hawks, and other birds. Automobiles contribute to the death rate of many turtles, especially adults. Overall, raccoons are often assumed to be the major predator.

In our model, painted turtles have three age classes: hatchlings (1 year old), juveniles (2–7 years old), and adults (4–8+ years old). During the first year after emergence from the nest, hatchling growth is very rapid, and they may double in size. Juveniles grow at a steady rate until maturity is reached. Growth is much slower after maturity begins. Males reach maturity after 1–5 years, while females require 5–9 years. Painted turtles in northern climates reach maturity later than those in southern climates. Male painted turtles generally live for at least 6 years, and females generally have a life span of at least 12 years. Many of both gender live for 15 years, and it has been reported that some may survive for 30–40 years. However, the upper limit on life span is unknown.

Reproduction occurs in late May through mid-July. Temperature strongly influences the beginning of the nesting season, although how temperature determines the beginning may depend on the location. Reports in Quebec suggest the beginning is positively correlated with the average previous year's temperature. But, in the Nebraska sandhills, the onset of nesting is inversely correlated with the average maximal temperature in March through May of the current year, and the previous year's temperature is unrelated to the onset of nesting. In Michigan, the onset of nesting is most strongly affected by the temperatures in May of the current year. Most nests are constructed in the late afternoon or early evening. Nests are dug in sandy soil and are flask shaped. Usually, nests are dug within 200 m of water, but may be as far away as 600 m. After depositing and covering the eggs with soil, the female often wets the soil with bladder water. The nests are frequently dug out in the open where it is exposed to direct sunlight. If weather conditions are not favorable, either too hot or too dry, the female may delay nesting for up to 3 weeks, with differences among subspecies and location.

Female painted turtles store sperm of their mates. They can use this sperm to fertilize multiple clutches within a single season and over multiple seasons. Females may also mate with another male even if they have stored sperm from previous copulations. In this case, the most recent sperm is used in fertilizing the eggs first. Larger clutches have a higher frequency of multiple paternity than smaller clutches (Pearse et al., 2001, 2002). This life history characteristic introduces a difficult modeling issue that we address later and take into account in our model.

Eggs pass through a total of 26 different development stages. The first 8 stages last approximately 1 day, while the later stages last up to a week. For example, stage 17 lasts about 1 week, and during this time the lower jaw begins to grow, the forelimb's digits are noticeable but not distinct; the carapace's central and lateral laminae are distinctly demarcated, but the marginal laminae are not (Yntema, 1968).

Both the rate at which the soil conducts heat and the level of humidity play a role in the hatching rate of the eggs. Eggs incubated in moist soil tend to take longer to hatch but have a greater hatching rate than those in dryer soil. Also, eggs incubated in soil with higher thermal conductivity absorb more water than those incubated in soil with lower thermal conductivity (Ernst et al., 1994).

Eggs hatch, on average, after a 76-day incubation period (Ernst et al., 1994). In colder climates the turtles overwinter in the nest and emerge in the spring. Turtles have the ability to be frozen in the nest over winter and can survive temperatures as cold as −8.9 °C. Cagle (1954) reports that during the first 10 days after emergence from the eggs, the turtles change greatly in appearance, and by the 10th day they take on the size and proportions of small juveniles.

According to Gibbons (1968) there are three principal causes of nest failure: infertility (the eggs are not viable and will not hatch), environmental conditions (such as extreme heat, cold, moisture, or dryness), predation (mainly by raccoons, but also by other small rodents, foxes, snakes and even humans).

As we noted, temperature determines the sex of the turtles. Eggs incubated between 22 and 28 ° C produce only male turtles, and eggs incubated between 19–22 and 28–32 ° C produce only female turtles. Incubation at intermediate temperatures produces turtles of both sexes. Maleness is determined earlier in development than is femaleness. If the incubation temperature is 25 ° C from time of laying to stage 16, males will develop, but incubation at 31 ° C is required from laying until stage 22 for females (Ernst et al., 1994). There is no evidence that females select nest locations to influence the sex of the clutch (Ernst et al., 1994).

The age of a turtle can be determined for hatchlings and juveniles by counting the number of plastral annuli. However, as turtles mature these annuli become less pronounced and are more difficult to count. Therefore, determining the exact age of an adult turtle is difficult. It is generally assumed that males reach maturity once they have reached a plastron length of greater than 80 mm, which occurs after 1–5 growing seasons, while females do not reach maturity until their plastron length is greater than 115 mm, about 5–9 seasons. Females grow faster and larger than males.

The authors' participation in field experiments near Cedar Point Biological Station in western Nebraska during the last few years confirm many of these observations. Mark-and-recapture experiments gave survival and development information, and X-ray analysis of gravid females led to information about maternity and clutch size; diet was determined from stomach contents. The detailed results are not yet published, waiting for additional long term data collection. But one certain observation is that nest loca-

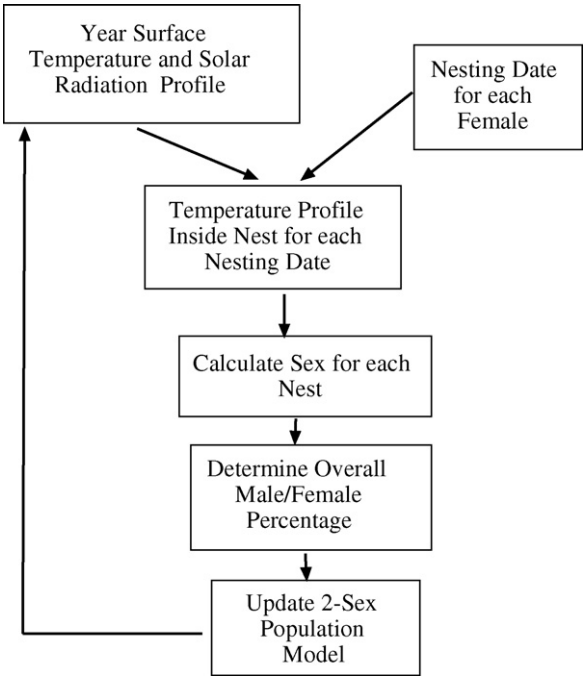

Fig. 2. A flow chart of the model's yearly dynamics.

tions and hatchling populations are difficult to determine, giving reasons for the wide discrepancy shown in others' mortality estimates in the early stages of development.

1.3. Population dynamics

Our goal is to formulate a computational model to examine effects of climate change on painted turtle populations. Such a model's complexity puts it beyond the reach of mathematical analysis (e.g., Ellner and Guckenheimer, 2006, p. 243) because it contains a large number of interacting processes and a large parameter set. Each part, or agent, of the model is modeled explicitly with a set of rules governing the interactions between the agents. Because of their complexity, these models are analyzed by computer simulation. A criticism of this type of a model is that one is replacing a complex biological process with a complex computer algorithm. However, a computer analysis has its benefits because it can be studied in a much shorter amount of time than the actual biological system, and biological systems often do not provide the luxury of offering opportunities for numerous experimental observations. A mathematical model allows the researcher to change parameters without disturbing the actual system. Another criticism is that because the models are complex, it is difficult to determine exactly why an outcome occurs. While this criticism cannot be fully remedied, we usually perform a sensitivity analysis on the parameters, where one considers small perturbations of each parameter while holding the others fixed. This allows the researcher to rank parameters in order of impact and it often aids in the implementation of biological experiments. The goal of such a model is not to obtain exact population sizes, but to determine how much a parameter change causes a population changes from a baseline case. This common research approach is in the true spirit of mathematical modeling, as has been expressed eloquently by Ellner and Guckenheimer (2006) and Maynard Smith (1974).

In the overall population model, there are four principal parts (see Fig. 2):

1. Input of stochastic daily temperature and solar radiation profiles.
2. Solving a heat transfer problem to determine the nest temperature profiles, especially in the egg layer.
3. Calculating the consequent sex ratio of the nest using a degree-day model.
4. Formulating and numerically solving a discrete time, two-sex, stage-based model of population dynamics for the male and female turtle populations.

We increment the model yearly. That is, in each year we first input stochastic temperature and solar radiation profiles. For each female in the population, we determine a nesting date. Next we calculate the temperature profile inside the egg layer in each nest from the classical heat, or diffusion, equation with a radiation boundary condition. From this we determine the sex ratio of the nest using a degree-hour approach, finally updating the population projection matrix. We repeat this process for a 30-year time period.

2. Nest temperature

Almost all studies of TSD, both experimental and theoretical, were conducted in the egg layer at constant temperature levels. In our model we use variable environmental temperatures and solar radiation, and we calculate temperatures in the egg layer using a classical diffusion model. We make several assumptions to simplify the diffusion model for temperatures in the nest.

1. Heat flow occurs only in the vertical, or downward, direction. Because of model complexity, we do not consider detailed lateral geometry of the nest. The replaced soil in the top of the nest is assumed to have the same conductivity (and therefore, packing characteristics and porosity) as the undisturbed soil.
2. The metabolic heat created by the eggs is negligible. In a study on parchment-shelled reptile eggs, such as for the painted turtle, Ackerman et al. (1985b) found that the eggs of three species of reptiles would be, on average, 0.18 ◦ C warmer than the air temperature. Because the clutch size of the painted turtle is small (say, much less than 20 eggs) (Ernst et al., 1994; Iverson and Simith, 1993), and because the temperature increase is minimal, we do not include the metabolic heat created by the eggs as a source term in the diffusion equation for determining nest temperatures. This assumption would not be valid for species of reptiles that have large eggs or clutches, such as the sea turtle Crouse et al. (1987). This assumption is consistent with the assumption of no lateral heat flow.
3. Moisture levels in the nest remain constant. Water potential inside the nest is important for embryonic survival (Ackerman et al., 1985a,b; Cagle et al., 1993; Gutzke et al., 1987; Rimkus et al., 2002), and we assume that the moisture level remains constant and sufficient for development. This assumption implies no large rain events. This assumption simplifies the model in that the diffusivity of the soil and egg layers remain constant instead of variable (moisture dependent).
4. The thermal conductivity of the egg layer is computed as a weighted average of that of eggs and air. The eggs are modeled as ellipsoids, and the amount of air in between the eggs is found from a packing relation for ellipsoids. The soil above the egg layer, though it has been removed and replaced by the turtle, is assumed to be the same as the undisturbed soil.
5. The only stochastic environmental effects are ambient temperature and solar radiation. While other aspects of environmental stochasticity (e.g., predators, food availability) may impact turtle mortality and egg production, we consider only abiotic weather effects.

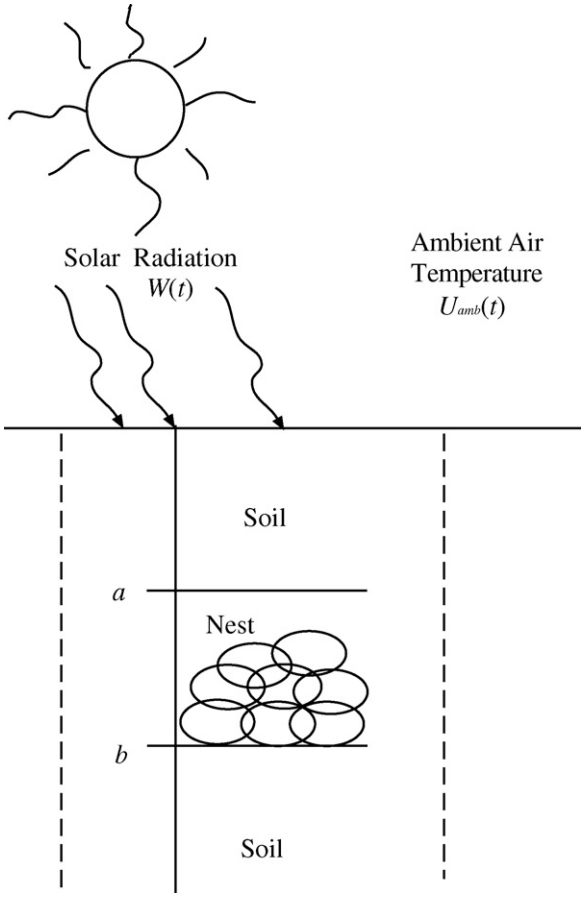

Fig. 3. Schematic of a turtle nest below a ground area A. The egg layer is located at $a \le x \le b$, where x is the depth below the surface $x = 0$.

2.1. Diffusion equation for the nest

A diagram of the nest setup is shown in Fig. 3. We begin by setting up the heat equation governing the flow of heat downward through the nest, along with the corresponding boundary conditions on the surface and at the top and bottom of the nest. Finally, we formulate a numerical algorithm using a finite difference scheme to obtain approximate solutions for this part of the model.

The flow of heat downward through the nest is governed by the classical diffusion, or heat, equation, with depth $x = 0$ at the surface. See, for example, Logan (1987). We assume the egg layer begins at depth $x = a$ and ends at depth $x = b$, with $0 < a < b$. Let $u(x, t)$ be the temperature at depth x at time t, and let A be the cross-sectional area of the nest. Then at any depth x within the nest, the heat flux at x is given by Fourier's Law

$$\text{flux at } x = -K(x)u_x(x, t),$$

where

$$K(x) = \begin{cases} K_s, & 0 \le x < a \text{ and } x \ge b \\ K_e, & a \le x < b \end{cases}$$

is the thermal conductivity in the soil and egg layers. Let

$$c(x) = \begin{cases} c_s, & 0 \le x < a \text{ and } x \ge b \\ c_e, & a \le x < b \end{cases},$$

$$\rho(x) = \begin{cases} \rho_s, & 0 \le x < a \text{ and } x \ge b \\ \rho_e, & a \le x < b \end{cases}$$

be the specific heat and density, respectively, with subscripts denoting the values in the soil and egg layers. It follows from the basic conservation of energy law that

$$u_t(x, t) = \frac{1}{c(x)\rho(x)} \frac{d}{dx}(K(x)u_x(x, t)),$$

which is the heat equation for a nonhomogeneous medium with no heat sources. Because c, ρ, and K are constant in each zone (soil or egg layer), we can write

$$u_t = k(x)u_{xx}, \tag{1}$$

where

$$k(x) = \frac{K(x)}{c(x)\rho(x)}$$

is the diffusivity. By constancy of the parameters,

$$k(x) = \begin{cases} k_s, & 0 \le x < a \text{ and } x \ge b \\ k_e, & a \le x < b \end{cases},$$

where $k_s = \frac{K_s}{c_s\rho_s}$ and $k_e = \frac{K_e}{c_e\rho_e}$.

Next we formulate the conditions at the boundaries: the surface, the soil–egg layer interfaces, and the lower boundary. At the ground surface $x = 0$, the net heat flux into the soil must equal to the flux due to the temperature difference between the surface and the ambient air temperature plus the flux due to solar radiation. From Fourier's law, the flux into the ground at $x = 0$ is

$$-AK_s u_x(0^+, t),$$

and the flux due to temperature differences is

$$Ah(U_{\text{amb}}(t) - u(0^+, t)),$$

where h is the heat transfer coefficient from Newton's law of cooling, and $U_{\text{amb}}(t)$ is the ambient air temperature at time t. The radiation flux is

$$A\alpha W(t),$$

where $W(t)$ is the solar radiation at time t, and α is the proportion of the solar energy absorbed by the soil. Putting this all together, we have

$$-AK_s u_x(0^+, t) = Ah(U_{\text{amb}}(t) - u(0^+, t)) + A\alpha W(t),$$

or

$$u(0^+, t) - \frac{K_s}{h}u_x(0^+, t) = U_{\text{amb}}(t) + \frac{\alpha}{h}W(t). \tag{2}$$

This is a classical radiation boundary condition.

The standard condition at a soil–egg layer interfaces is: the heat flux is continuous across the interfaces. That is, the interface conditions are

$$K_s u_x(a^-, t) = K_e u_x(a^+, t), \qquad K_e u_x(b^-, t) = K_s u_x(b^+, t). \tag{3}$$

In the model we assume that the temperature profile is known at some fixed depth L. That is,

$$u(L, t) = \text{const}. \tag{4}$$

This is a reasonable assumption because the earth's temperature is relatively constant at $L = 9.76$ m below the surface (Anon., 2010). Note that this depth is much greater than that of the nest, which is between 8 cm and 12 cm below the surface.

Eqs. (1)–(4) form the boundary value problem (BVP) for the temperature in the nest for $0 < x < L$, $t > 0$. It is not shown here, but this BVP, subject to an initial condition on the temperature $u(x, 0)$, has a unique solution and is therefore a well posed problem.

2.2. Discrete temperature approximation

An analytic solution of the BVP is beyond the scope of tractability, and we therefore use a numerical algorithm to find approximate solutions. We apply a backward implicit method because of convergence for all choices of temporal step size (e.g., see, Logan, 1987).

In a standard way we set up a grid (x_j, t_n), $j = 1, 2, \ldots, J$, $n = 1, 2, \ldots, N$, of lattice points with $t_1 = x_1 = 0$, and $x_{j+1} = x_j + \Delta x$, $t_{n+1} = t_n + \Delta t$. (Note that the counter starts at 1, instead of the conventional 0, to be consistent with array notation required in MATLAB.) Then, $u(x, t) \approx U(x_j, t_n)$ for some j, n, and for simplicity we write $U(x_j, t_n) = U_{j,n}$. The implicit method uses the backward approximation for the time derivative and a centered difference approximation for the second spatial derivative, or

$$u_t \approx \frac{U_{j,n} - U_{j,n-1}}{\Delta t}, \qquad u_{xx} \approx \frac{U_{j+1,n} - 2U_{j,n} + U_{j-1,n}}{(\Delta x)^2}.$$

Thus, to leading order, the heat Eq. (1) is approximated by the difference equation

$$\frac{U_{j,n} - U_{j,n-1}}{\Delta t} - k(x)\frac{U_{j+1,n} - 2U_{j,n} + U_{j-1,n}}{(\Delta x)^2} = 0,$$

which simplifies to

$$-rU_{j-1,n} + (1 + 2r)U_{j,n} - rU_{j+1,n} = U_{j,n-1},$$

where $r = k(x_j)\Delta t/(\Delta x)^2$. This is a system of equations for $U_{j,n}$ ($j = 1, \ldots, J$) for each fixed time n, and we write it in matrix form as

$$\begin{bmatrix} U_{1,n-1} + rU_{0,n} \\ U_{2,n-1} \\ \vdots \\ \vdots \\ U_{J-2,n-1} \\ U_{J-1,n-1+rU_{J,n}} \end{bmatrix} = \begin{bmatrix} 1+2r & -r & & & & \\ -r & 1+2r & -r & & & \\ & -r & \ddots & \ddots & & \\ & & \ddots & \ddots & \ddots & \\ & & & & -r & \\ & & & -r & 1+2r & \end{bmatrix} \begin{bmatrix} U_{1,n} \\ U_{2,n} \\ \vdots \\ \vdots \\ \vdots \\ U_{J-1,n} \end{bmatrix}. \tag{5}$$

Note that $U_{0,n}$ are values on an inserted false boundary. The computational molecule is shown in Fig. 4. To implement the scheme, at each time step we solve this linear system to obtain the values of the temperature at each depth lattice value at that time.

Extreme care is required to approximate the radiation boundary condition (2). We have $u(0+, t) \approx U_{1,n}$ and $u_x(0+, t) \approx (U_{2,n} - U_{0,n})/2\Delta x$. It is important to discern that $U_{0,n}$ refers to the *false* boundary values and *not* to the ambient air temperature above the ground. We then obtain

$$U_{1,n} - \frac{K_s}{h}\left(\frac{U_{2,n} - U_{0,n}}{2\Delta x}\right) = U_{\text{amb}}(t_n) + \frac{\alpha}{h}W(t_n),$$

or

$$U_{0,n} = \frac{1}{\beta}\left(U_{\text{amb}}(t_n) + \frac{\alpha}{h}W(t_n) - U_{1,n}\right) + U_{2,n}, \tag{6}$$

where $\beta = K_s/2h\Delta x$. The first row in the matrix Eq. (5) is

$$U_{1,n-1} + rU_{0,n} = (1 + 2r)U_{1,n} - rU_{2,n}.$$

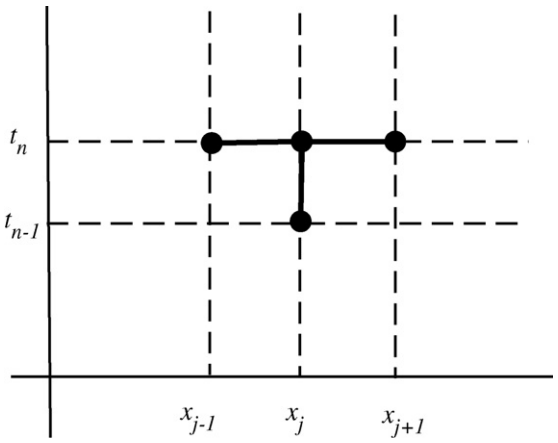

Fig. 4. The computational molecule for the implicit scheme. To handle flux boundary conditions, a false boundary is inserted just above ground level, at $x = x_0 = -\Delta x$; $x = 0$, the surface, corresponds to x_1.

Using (6), we then have

$$U_{1,n-1} + \frac{r}{\beta}\left(U_{\text{amb}}(t_n) + \frac{\alpha}{h}W(t_n)\right) = \left(1 + 2r + \frac{r}{\beta}\right)U_{1,n} - 2rU_{2,n}.$$

At the lower boundary, or at depth $L = x_J$, we have that $u(L, t) = g = \text{const}$. Therefore we set $U_{J,n} = g$ for all n.

Recall that the conditions at the interfaces, or at the top and bottom of the egg layer, require that the flux is continuous. This implies

$$-K_s\left(\frac{U_{a,n} - U_{a-1,n}}{\Delta x}\right) = -K_e\left(\frac{U_{a+1,n} - U_{a,n}}{\Delta x}\right) \tag{7}$$

and

$$-K_e\left(\frac{U_{b,n} - U_{b-1,n}}{\Delta x}\right) = -K_s\left(\frac{U_{b+1,n} - U_{b,n}}{\Delta x}\right). \tag{8}$$

Here, a and b depend upon the location of the egg layer as well as the choice of step size. In the model we use values for Δx so that a and b are lattice points in the discretization. Hence, from Eqs. (7) and (8), at depths a and b the corresponding rows in the matrix equation are

$$K_sU_{a-1,n} - (K_s + K_e)U_{a,n} + K_eU_{a+1,n} = 0,$$
$$K_eU_{b-1,n} - (K_s + K_e)U_{b,n} + K_sU_{b+1,n} = 0.$$

2.3. The input temperature

The daily, ambient, stochastic temperature profile, which is an input into the model, is generated by the autoregressive process given in Logan and Wolesensky (2007); see also Logan et al. (2006). The temperature profile, $\theta_y(t)$, for each Julian day, y, is given by the sinusoidal curve

$$\theta_y(t) = \Theta_y - \phi_y \cos\left(\frac{\pi}{12}(4 - t)\right),$$

where $0 \le t < 24$. Here Θ_y is the stochastic average daily temperature and ϕ_y is the stochastic daily amplitude. The average daily temperature is given by

$$\theta_{avg}(y) = Y_{avg} - Y_{amp}\cos\left(\frac{2\pi}{365}(35 - y)\right),$$

where Y_{avg} is the yearly average temperature and Y_{amp} is the yearly average amplitude and y is the Julian day of the year. Then, the stochastic daily temperature is given by the auto regression

$$\Theta_{y+1} = \theta_{avg}(y) + Y_{cor}(\Theta_y - \theta_{avg}(y)) + \sigma_y\sqrt{1 - Y_{cor}^2}Z$$

where Y_{cor} is the autocorrelation of the current day's temperature with the previous day's temperature, σ_y the standard deviation of the temperature and Z a normal random variable with mean 0 and standard deviation 1.

The temperature amplitude for each day is determined by

$$\phi_{y+1} = Y_{amp} + \Phi_{cor}(\phi_y - Y_{amp}) + \sigma_\phi \sqrt{1 - \Phi_{cor}^2} Z$$

where Φ_{cor} is the autocorrelation of the current day's amplitude with the previous day's amplitude and σ_ϕ is the standard deviation of the amplitude.

The baseline values used for the temperature profile are:

$$Y_{avg}=10,\ \ Y_{amp}=13.5,\ \ Y_{cor}=.9,\ \ \sigma_y=4.4,\ \ \Phi_{cor}=.9,\ \ \sigma_\phi=4.4,$$

which models temperatures collected at the weather station at Cedar Point Biological Station.

We use average monthly data from the National Renewable Energy Laboratory (Radiation, 1994) to calculate the daily solar radiation. We assume that the solar radiation is zero between the hours of 8:00 pm and 6:00 am. We assume the most intense rays occur at 2:00 pm. We model the daily solar radiation by a piecewise cubic equation

$$W(t) = \begin{cases} 0, & 0 \le t \le 6 \text{ and } 18 \le t < 24, \\ At^3 + Bt^2 + Ct + D, & 6 \le t \le 18. \end{cases}$$

For each Julian day y we choose a value r_y from a uniform distribution between 0 and 0.8 to be the maximum solar radiation given in W/cm^2, where 0.8 was determined from solar radiation data in Nebraska (Radiation, 1994). Because $W(t)$ must pass through the points, $(6, 0)$, $(14, r_y)$, and $(20, 0)$ with maximum at $(14, r_y)$, we can solve for the coefficients of the cubic. In our model we have not correlated the daily temperature to the solar radiation.

We combine the models in the previous sections together to examine the dynamics in the turtle population based upon various changes in the temperature profile. A flow chart of this process was shown in Fig. 2.

Each year, we determine the temperature and solar radiation profiles. We choose a first nesting date for each female from a truncated-normal random distribution, with mean June 1 and standard deviation of 7 days. The distribution is truncated at May 1 and June 30. These dates are given in Iverson and Simith (1993), and are similar to those in Rowe et al. (2003). According to Iverson and Simith (1993), the second nest occurs, on average, 16 days after the first nest. Thus, we assume that the turtle lays a second nest 16 days after her first nest. Next, we calculate the temperature profile inside the nest for each nesting episode. Once we have determined the temperature profile inside the nest, we then use the degree hour model to find the sex of each nest. We then calculate the overall sex ratio for the eggs that year by averaging the outcomes of each nest. We finally update the population projection model.

We repeat this process for a period of 30 years, and observe the outcome of the population vector. We repeat this process for 100 total runs for each change in the temperature model. After the baseline runs, we increase the average temperature by 2 ° C and then 4 °C. We also observed the change in the dynamics when we change the daily amplitude variation. We chose to observe the effects of changing average temperature and daily amplitude because Shine and Harlow (1996) found, for skinks (*Bassiana duperreyi*), that both the mean temperature and the temperature variance influenced development rates and thus incubation periods.

Finally, we compare the numerical solution for the temperature in the nest and experimental SCAN data gathered from Roger's farm (NRCS, 2010) as input for the ambient temperature and radiation. We compared the calculated result using the diffusion model at 10 cm below the surface to the data taken with temperature sensors

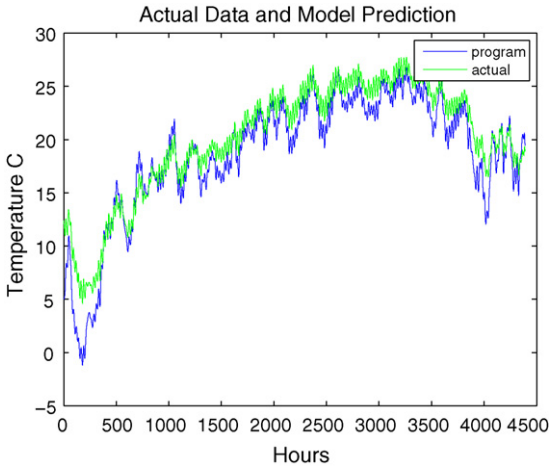

Fig. 5. Actual temperature data taken from Roger's Farm compared to the numerical approximation at 10 cm below the surface.

at the farm. Because the data from Roger's farm does not include a nest, we assumed that the nest in the numerical simulation began and ended at the same depth of 9.14 m. Both the experimental and computed temperature profiles are shown in Fig. 5. Overall, the numerical solution closely approximates the experimental temperature profile. However, when there are large changes in the surface temperature, the numerical solution seems to slightly exaggerate these changes. Episodes of rain are not included in the numerical model, which may also explain some of the differences in the two profiles.

The egg layer parameters (diffusivity) for the calculation were given with the experimental data, and we used the Nelder–Mead algorithm in Matlab to determine the remaining thermal parameters (the heat absorption coefficient and diffusivity of the soil layers).

3. Sex ratio of the clutch

The assumption is that each adult female turtle nests twice a year and produces a nest every year. Iverson and Simith (1993), report that painted turtles in Nebraska generally produce two nests each year. As we noted in Section 1.2, there is no indication that there is an upper limit on reproduction age; Wilbur (1975a) records gravid, nesting females over 30 years of age.

Recall that painted turtles have two thresholds for determining sex. Nests produce exclusively males if the eggs are incubated between 22 ° C and 28 °C. Eggs incubated at temperatures below 22 ° C or above 28 ° C produce females (see Fig. 1). However, if the temperature fluctuates about one of these thresholds, a mixed nest will be produced (Gutzke and Paukstis, 1984; Schwarzkpf and Brooks, 1985). Schwarzkopf and Brooks (1987) found that degree hours best predicted the sex of the nest. Thus, we determine the sex of each nest based upon the proportion of development achieved within each temperature range.

Let $d(\theta)$ be the development rate, given in degree-days per day, at temperature θ. Note that θ is a function of time t. Then, the total development, from time $t = 0$ to $t = t^*$ is given by

$$\int_0^{t^*} d(\theta(t))dt.$$

We assume that the development rate is linear, and we use data from Cagle et al. (1993) and Gutzke et al. (1987) to parameterize the development function. Following the method in Shine and Harlow (1996), we divide the shortest incubation time (41 days) by the incubation time for each temperature (Table 1). We then calculated

Table 1
The incubation period is the number of days until pipping. Data from Gutzke et al. (1987) has temperature readings of 22, 27 and 32, with other readings from Cagle et al. (1993).

Temperature (°C)	Incubation period (days)	Development rate
22	97.9	0.4188
22	97.9	0.4188
22	100	0.41
23.4	72.3	0.5671
23.6	68.7	0.5968
23.6	65.4	0.6269
23.9	66.9	0.6129
24	68.8	0.5959
24.7	60.6	0.6766
24.8	56.3	0.7282
26	57.8	0.7093
26.2	61.1	0.671
27	53.5	0.7664
27	52.7	0.778
27	51.4	0.7977
32	45.4	0.9031
32	42	0.9762
32	41	1

the least squares regression line with these points ($R^2 = 9075$). Thus, the development function is

$$d(\theta) = \begin{cases} .05\theta - .6068, & 12.136 \geq \theta \\ 0, & \theta < 12.136 \end{cases}.$$

To determine the thermal sensitive period, we determine the starting time, TSP_{begin}, and the ending time, TSP_{end}, of the middle third of the development period by solving

$$\int_0^{TSP_{\text{begin}}} d(\theta(t))dt = 0.\overline{33}$$

and

$$\int_0^{TSP_{\text{end}}} d(\theta(t))dt = 0.\overline{66}$$

for TSP_{begin} and TSP_{end}, respectively.

We do this numerically by calculating the sum

$$\sum_{n=0}^{n^*} d(\theta(t_n))\Delta t,$$

where Δt is the time increment between time t_n and t_{n+1}, until we have reached one-third and two-thirds of the total development, respectively.

Next we determine the proportion of development within each temperature range. Let $\Theta = [\theta_1, \theta_2]$ be a temperature interval and $\mathfrak{T} = [TSP_{\text{begin}}, TSP_{\text{end}}]$. Then, numerically, the total development achieved within that range is given by

$$\sum_{\{t \in \mathfrak{T}: \theta(t) \in \Theta\}} d(\theta(t))\Delta t.$$

We then compare the total development in the female range, the male range, and the mixed range. The range that has the highest cumulative development gives the sex ratio of the nest. Note that we are combining the total development in both female temperature ranges together and the development in both of the mixed ranges together when determining the sex of the nest. If the largest proportion of development is in the male temperature range, the algorithm deems that nest to be male and returns 0 as the proportion of females. If the largest proportion of time is spent in the mixed range, the model returns 0.5 as the proportion of females, and if the proportion is in the female range, it returns the value 1. We calculate this proportion for each nest laid and average the results for the year to determine the overall ratio of male to female eggs.

4. Population model

We model population dynamics of the system with a two-sex model. The reasons are twofold. First, males reach maturity faster than females. Males reach maturity after 1–5 years, while females require 5–9 years (Gibbons, 1968; Ernst et al., 1994). Second, besides being polyandrous, female turtles also store the sperm of their mates (Pearse and Avise, 2001; Pearse et al., 2002). They use this sperm even if they mate again the subsequent year, employing a "last in first out" fertilization scheme (Pearse and Avise, 2001; Pearse et al., 2002). That is, they use the most recent sperm first and then the stored sperm. In a population, it is possible that reproduction could be sperm-limited if the temperature increase leads to female dominated population. Once the ratio of adult males to adult females is less than 1:2, the number of eggs declines dramatically. The ratio of adult males to adult females is generally 1:1, although skewed sex ratios of 1.36:1 (male dominate) and 1:1.39 (female dominate) have been reported (Ernst et al., 1994, p. 295).

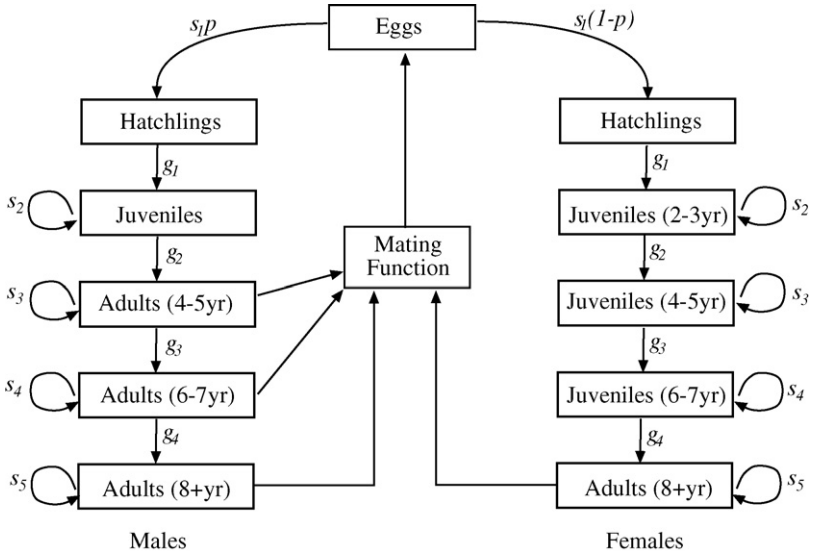

Fig. 6. Two-sex model of a painted turtle population, incremented yearly.

The life cycle graph of the system is shown in Fig. 6. In this model, turtles are divided into five age classes. Because of the variability of the age at maturity, we could have done a stage structured model instead. However, according to Iverson and Simith (1993), "age and size at maturity are about equally variable". Because painted turtles in northern climates reach maturity later than those in southern climates (Iverson and Simith, 1993; Wilbur, 1975a), we use the later ages for reaching adulthood. For males the classes are hatchlings (year 1), juveniles (years 2–3) and three adult stages, 4–5 years, 6–7 years and 8+ years. For females the classes are hatchlings (year 1), three juvenile classes, 2–3 years, 4–5 years and 6–7 years, and adults. Recall that in northern climates, the painted turtle eggs are laid from May to mid July and the turtles overwinter in the nests emerging in the spring, so we give them their own age class (Ernst et al., 1994).

We set s_i, $i = 1, \ldots, 5$ and g_i, $i = 1, \ldots, 4$ to be the survivorship and graduation rates, respectively, and p is the proportion of eggs that are male. The annual survivorship of both males and females is similar within each age class (Heppell, 1998; Mitchell, 1988; Tinkle et al., 1981). Thus, we assume that the survivorship and graduation rates are the same for males and females within an age class. Note that s_1 and s_5 represent true annual survivorship rates, but s_2, s_3 and s_4 are not true annual survivorship rates because the turtles remain in the age classes they represent for 2 years.

We define the variables E, eggs, H_m and H_f, male and female hatchlings, $J_m, J_{f1}, J_{f2}, J_{f3}$, male and female juveniles, A_{m1}, A_{m2}, A_{m3}, A_f, male and female adults. Each variable is a function of time. That is, $J_{f1}(n)$ is the number of female juveniles age 2–3 years at year n. From Fig. 6, we deduce

$$
\begin{aligned}
H(n+1) &= s_1 pE(n),\\
J(n+1) &= s_2 J(n) + g_1 H(n),\\
A_{m1}(n+1) &= s_3 A_{m1}(n) + g_2 J(n),\\
A_{m2}(n+1) &= s_4 A_{m2}(n) + g_3 A_{m1}(n),\\
A_{m3}(n+1) &= s_5 A_{m3}(n).
\end{aligned}
$$

The female cycle is modeled similarly. In all, the equations can be written efficiently in matrix form as

$$
\begin{bmatrix} H_m \\ J_m \\ A_{m1} \\ A_{m2} \\ A_{m3} \\ H_f \\ J_{f1} \\ J_{f2} \\ J_{f3} \\ A_f \end{bmatrix} (n+1)
= \begin{bmatrix}
s_1 p & 0 & 0 & 0 & 0 & 0 & 0 & 0 & 0 & 0 \\
0 & g_1 & s_2 & 0 & 0 & 0 & 0 & 0 & 0 & 0 \\
0 & 0 & g_2 & s_3 & 0 & 0 & 0 & 0 & 0 & 0 \\
0 & 0 & 0 & g_3 & s_4 & 0 & 0 & 0 & 0 & 0 \\
0 & 0 & 0 & 0 & g_4 & s_5 & 0 & 0 & 0 & 0 \\
s_1(1-p) & 0 & 0 & 0 & 0 & 0 & 0 & 0 & 0 & 0 \\
0 & 0 & 0 & 0 & 0 & 0 & g_1 & s_2 & 0 & 0 \\
0 & 0 & 0 & 0 & 0 & 0 & 0 & g_2 & s_3 & 0 \\
0 & 0 & 0 & 0 & 0 & 0 & 0 & 0 & g_3 & s_4 \\
0 & 0 & 0 & 0 & 0 & 0 & 0 & 0 & 0 & g_4 \; s_5
\end{bmatrix}
\begin{bmatrix} E \\ H_m \\ J_m \\ A_{m1} \\ A_{m2} \\ A_{m3} \\ H_f \\ J_{f1} \\ J_{f2} \\ J_{f3} \\ A_f \end{bmatrix} (n) \qquad (9)
$$

The population projection matrix is not square and does not give the number of eggs at time $n+1$. This is because the number of eggs at time n is determined by the number of adults at time n and number females at time $n-1$. We derive the egg equation later in a different format.

We assume that the annual survivorship rates within each age class is the same for the male and female populations. This is consistent with findings in the literature (Mitchell, 1988; Tinkle et al., 1981; Wilbur, 1975a). The values chosen for each age class are shown in Table 2. There is tremendous uncertainty in the annual survivorship for the eggs and hatchlings, mainly due to the difficulty in locating nests and counting the small hatchlings. We chose 0.33 for the eggs and 1 year old because it allows for the model to approach a stable equilibrium.

Table 2
Found in literature and used in model.

Age class	Tinkle et al. (1981)	Mitchell (1988)	Wilbur (1975a,b)	Model
Eggs and 1 year	0.67	0.19	0.08	0.33
2–3 years	0.76	0.46	0.82	0.6
4–7 years	0.76	0.94	0.82	0.7
8+ years	0.76	0.96	0.82	0.9

Table 3
For both males and females used in the matrix model.

Age class	Survivorship	Graduation
Egg and 1 year	0.33	0.33
2–3 years.	0.375	0.225
4–5 years.	0.4118	0.2882
6–7 years.	0.4118	0.2882
8+ years.	0.9	

We determine the survivorship and graduation rate for age classes that last for more than 1 year using the method given in Crouse et al. (1987) and Caswell (2001). We assume that the proportion of individuals in their first year in the age class is 1 and let q be the probability of surviving 1 year. Note that for each 2-year age class, q is the model proportion given in Table 2. Then, the relative abundance of individuals is $1+q$. Hence, the proportion of individuals in the first year of the age class is $1/(1+q)$, and therefore the probability of surviving and remaining in the age class is $q/(1+q)$. The proportion of individuals in their second year is $q/(1+q)$, and so the graduation probability is $q^2/(1+q)$. The survivorship and graduation rates used in the model are shown in Table 3.

The number of eggs $E(n)$ is determined by a mating function (see Caswell, 2001). We let $a_m(n)$ represent the sum of all adult males at time n. We assume that the number of mating episodes is the harmonic mean of the number of adult males and adult females. Although the harmonic mean was first used to model human populations, it has since been applied to many non-human populations (Engel et al., 2001; Lindström and Kokko, 1998; Ranta and Kaitala, 1999; Ranta et al., 1999; Sundelöf and Aberg, 2006). Thus, the total number of episodes is

$$\frac{2a_m(n)A_f(n)}{a_m(n)+A_f(n)}.$$

We next adjust the model to include the average number of eggs k laid by each female per year, and the number of females h mated with, per male. We get the total number of eggs laid each year:

$$E(n) = k\frac{2ha_m(n)A_f(n)}{ha_m(n)+A_f(n)}.$$

Finally, let r be the probability of using the sperm from the current year n, with $1-r$ the probability of using the sperm from last year. We are assuming that females do not store sperm for more than 1 year. Thus, the total number of eggs is the number of eggs fertilized from the current year's sperm plus the number of eggs fertilized from the previous year's sperm; therefore,

$$E(n) = r\frac{2a_m(n)kA_f(n)}{a_m(n)+h^{-1}A_f(n)} + (1-r)\frac{2a_m(n-1)kA_f(n-1)s_5}{a_m(n-1)+h^{-1}A_f(n-1)s_5}. \qquad (10)$$

We multiplied only the total number of females by the survivorship probability because to produce eggs in the current year they must be alive; but males do not need to be alive in the current year to use their sperm from the previous year. If we hold the number of females fixed, then the graph of the number of eggs vs. the number of males has the form of a saturated, type II functional response. Eq. (10) is a second-order difference equation, a fact that makes it unwieldy to include in a regular Leslie (Lefkovich) model.

In summary, we use a two-sex model because the males and females have different maturity rates and the females store sperm from 1 year to the next. The yearly dynamics are determined by the projection matrix (9) and the egg Eq. (10). Each year, we first calculate the number of hatchlings, juveniles and adults, and then we calculate the total number of eggs laid.

5. Simulations

Now we examine the behavior of the population under different temperature scenarios, holding other parameters fixed. Each simulation consists of 100 runs. First we simulate the population model with a fixed set of parameters and call this the *baseline simulation*. Then we change the temperature parameters and observe the resulting change in the population from the baseline. The average yearly temperature for the baseline simulation is 10 °C, and the average yearly amplitude is 13.75 °C. In the remaining scenarios, we increase the average temperature by 2 ° C and 4 °C, and for each we increase the amplitude by 0, 2, and 4 °C. For reference we denote each scenario by the temperature increase followed by the amplitude increase from the baseline run; for example, the simulation T4A2 has the average yearly temperature 4 ° C above the baseline temperature and the average yearly amplitude 2 ° C above the baseline amplitude. The median and the mean for each data set are approximately the same, differing at most by 43.24 individuals (occurring in T4A4, year 19) and on average differing by fewer than 14 individuals. For each scenario, two plots are shown. The first shows the total population average (not including eggs) as a solid line along with the 95% confidence interval as a dashed line about the average. (We assume that the data for each year is a *t*-distribution.) The second shows the average male (solid) and average female (dashed) population profiles. The output of the model over the first 5 years is similar in all cases because five iterations are required for the effects of the varying temperature profiles to transfer through all five age classes. We compute the growth rate for the total population average by calculating the geometric mean of the year-to-year growth rate (see Case, 2000). Growth rates are shown in Table 4. Some observations and implications suggested by model simulations can be summarized as follows (re: Figs. 7–15):

Table 4
The mean growth rate for each scenario.

Scenario	Growth rate
T0A0	0.999
T0A2	0.992
T0A4	0.996
T2A0	0.988
T2A2	0.995
T2A4	1.000
T4A0	0.993
T4A2	1.000
T4A4	0.979

1. In the baseline run (T0A0, Fig. 7), the growth rate is essentially 1. Small perturbations from the steady state decay, causing the population to return to the steady state. Hence, if the temperature trajectory remains at current levels, the turtle population will continue near the steady state (Fig. 7).
2. In the most severe case (T4A4), the average population growth rate is 0.979, which is not far from unity. This may imply a small buffering effect that contributes to the longevity of the species. One would expect a much lower birth rate.
3. In contrast to Janzen (1994), our model requires not only an increase of 4 °C, but also an increase in temperature variance of 4 °C. The case T4A4 is the only case where there may be a good possibility of long-time extinction (Fig. 13). In this case, about 95% of the simulations were at or below the steady state. Neither cases T4A0 nor T4A2 (Figs. 14 and 15) produced a growth rate small enough to consider it significant. In fact, the case T4A2 has growth rate of 1 (to three decimal places).
4. For *C. picta*, which has a temperature band selecting males, it is reasonable that strong temperature variations would adversely affect the population because radical changes means that the temperature will often be above or below the male range, giving female dominated populations. We recall that such temperature variations are predicted in many global change situations.

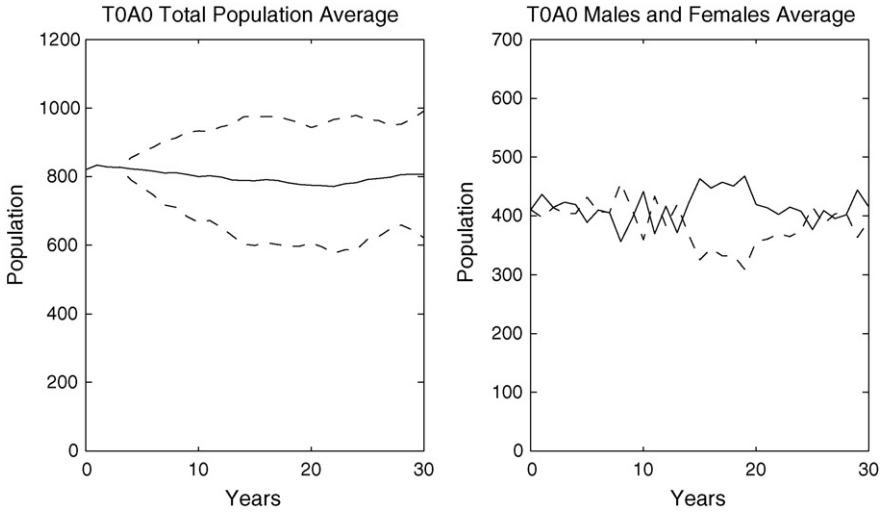

Fig. 7. Population profile for the *baseline* scenario (T0A0). The solid line represents the population average and average male population, respectively. The dashed line represents the 95% confidence interval and average female population, respectively.

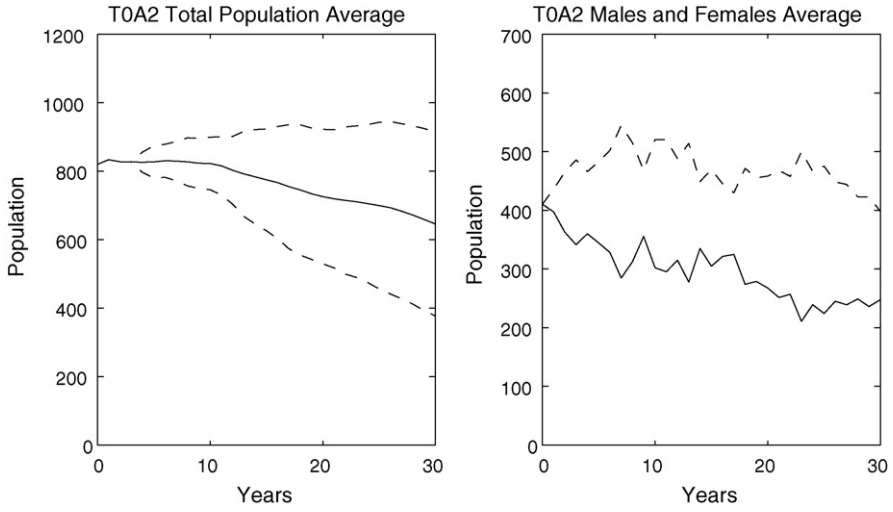

Fig. 8. Population profile for average yearly temperature 10 ◦ C and average yearly amplitude 15.75 ◦ C (T0A2). The solid line represents the population average and average male population, respectively. The dashed line represents the 95% confidence interval and average female population, respectively.

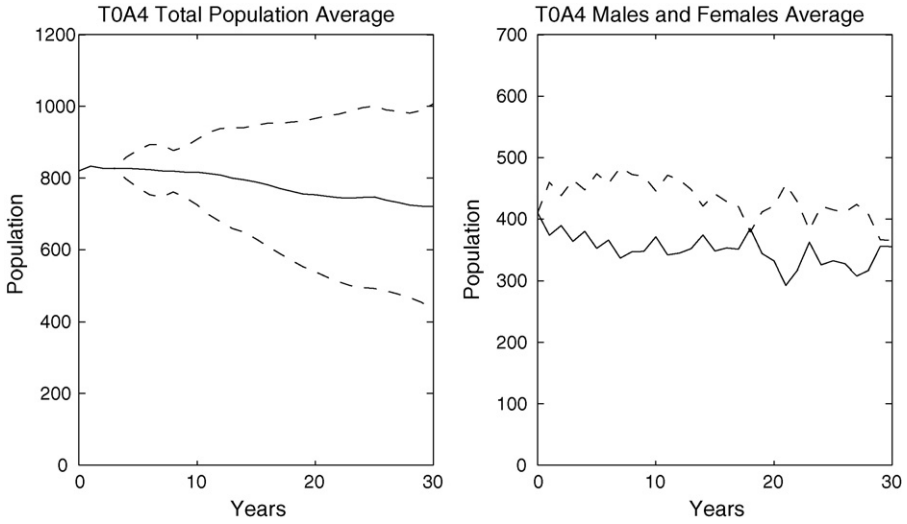

Fig. 9. Population profile for average yearly temperature 10 ◦ C and average yearly amplitude 17.75 ◦ C (T0A4). The solid line represents the population average and average male population, respectively. The dashed line represents the 95% confidence interval and average female population, respectively.

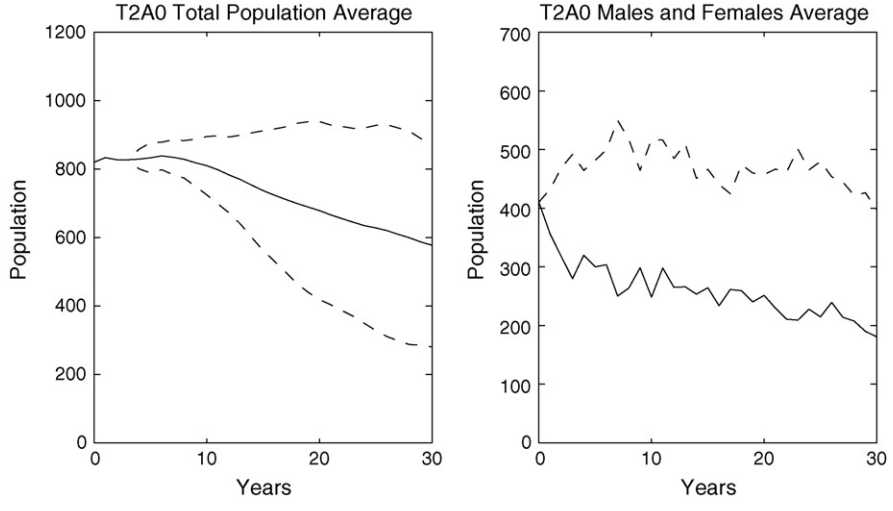

Fig. 10. Population profile for average yearly temperature 12 ◦ C and average yearly amplitude 13.75 ◦ C (T2A0). The solid line represents the population average and average male population, respectively. The dashed line represents the 95% confidence interval and average female population, respectively.

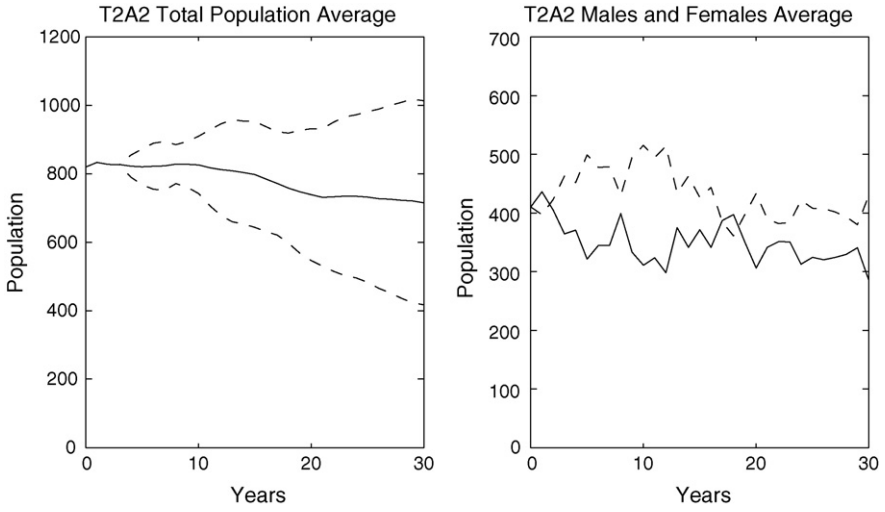

Fig. 11. Population profile for average yearly temperature 12 ◦ C and average yearly amplitude 15.75 ◦ C (T2A2). The solid line represents the population average and average male population, respectively. The dashed line represents the 95% confidence interval and average female population, respectively.

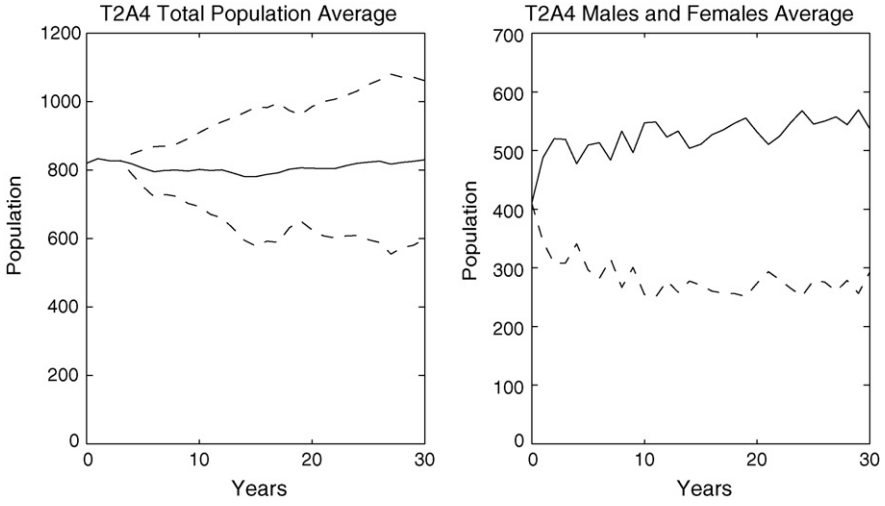

Fig. 12. Population profile for average yearly temperature 12 ◦ C and average yearly amplitude 17.75 ◦ C (T2A4). The solid line represents the population average and average male population, respectively. The dashed line represents the 95% confidence interval and average female population, respectively.

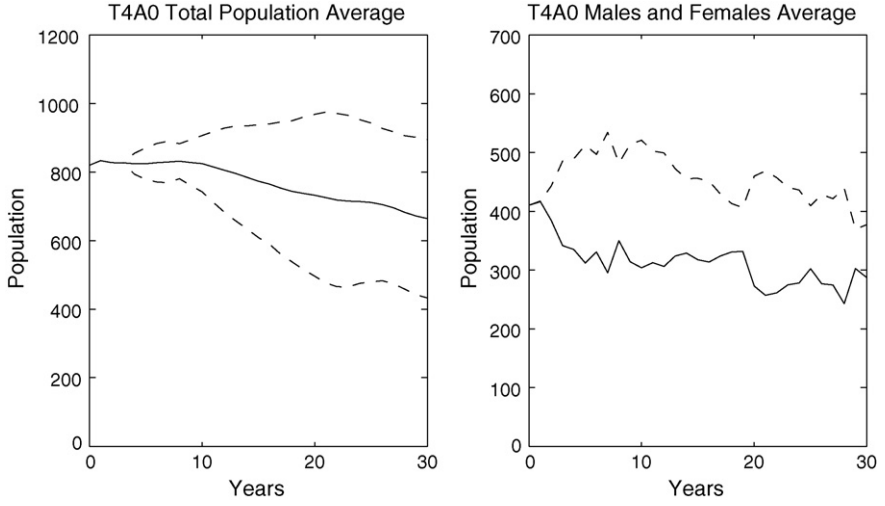

Fig. 13. Population profile for average yearly temperature 14 ◦ C and average yearly amplitude 17.75 ◦ C (T4A4). The solid line represents the population average and average male population, respectively. The dashed line represents the 95% confidence interval and average female population, respectively.

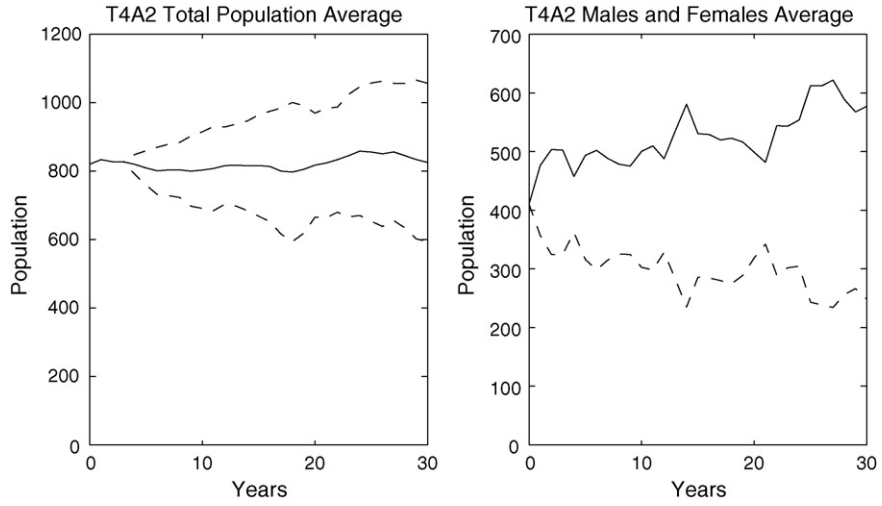

Fig. 14. Population profile for average yearly temperature 14 ◦ C and average yearly amplitude 13.75 ◦ C (T4A0). The solid line represents the population average and average male population, respectively. The dashed line represents the 95% confidence interval and average female population, respectively.

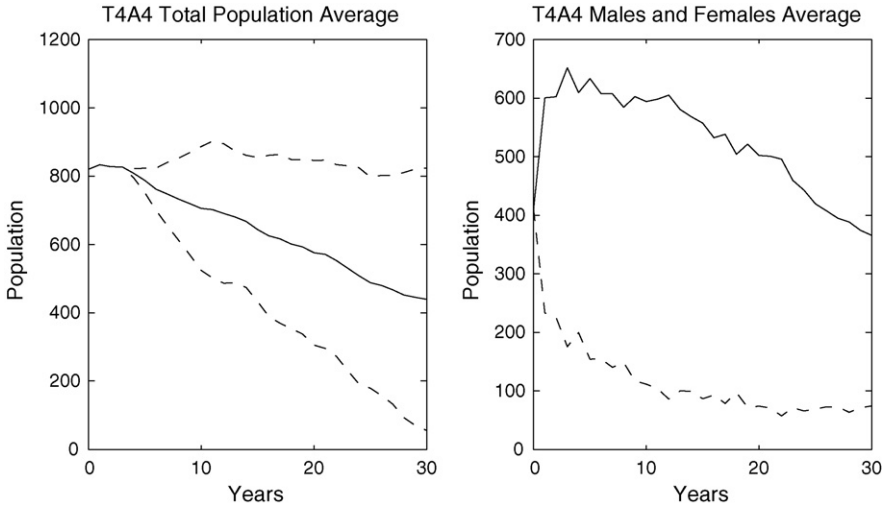

Fig. 15. Population profile for average yearly temperature 14 ◦ C and average yearly amplitude 15.75 ◦ C (T4A2). The solid line represents the population average and average male population, respectively. The dashed line represents the 95% confidence interval and average female population, respectively.

5.1. Parameter sensitivity

In model formulation and experimental designs, it is essential to know what are the crucial quantities and processes to include or to measure. One of the most important aspects of a computational model is that it gives information about the relative importance of the various parameters, and therefore, processes in the problem.

We examined the parameter sensitivity for the different portions of the model. The analysis is one-dimensional in the sense that we tested each parameter separately, varying it while holding the others fixed. For the ambient temperature we chose a fixed profile rather than random input for all the runs, which allowed us to discern the effects of each parameter with a minimum of noise. For the baseline simulation we set the ambient air temperature at $10\cos(\pi t/12) + 25$ (◦C) and the solar radiation at zero. For brevity and space limitations we do not show all the accompanying plots and tables, which detail the resulting changes from the results of the baseline simulation caused by incrementing the parameter values. Rather, we report the results in a narrative format. The change in the output was measured by the normed-difference between the baseline output and the altered output. For a time series, this norm is the maximum absolute value of the differences at each time step.

The baseline soil parameter values are shown in Table 5.

- *Soil conductivity*. For soil thermal conductivity we ran the model with K_s values between 9.3191 and 59.3191 W/cm h◦C, incrementing by 5 each on each run, which are values within the typical range of conductivities (Buonanno et al., 1995). All simulations produced temperatures within 3.29 ◦ C of the baseline temperature. As expected, the higher the soil thermal conduc-

Table 5
Parameter values in the nest temperature baseline simulation.

Parameter	Value
K_{soil}	14.6 W/(cm h ◦C)
K_{egg}	21.7875 W/(cm h ◦C)
$c_{soil}\rho_{soil}$	3.8 J/(cm^3 ◦C)
$c_{egg}\rho_{egg}$	1.7449 J/(cm^3 ◦C)

tivity of the soil, the greater the amplitude of the temperature variation.

- *Egg layer conductivity*. For the conductivity in the egg layer, we examined values 50% above and below the baseline value. Simulations produced temperatures within 0.19 ° C of the baseline value. The egg vs. air ratio in the layer was incremented between 15% and 75%, producing temperatures within 0.28 ° C of the baseline. These results show relative insensitivity to conductivities in the egg characteristics.
- *Density and specific heat*. The product of density and specific heat in the soil layer was incremented between 50% above and below the baseline product. Calculated temperature profiles were within 0.74 ° C of the baseline run. In the egg layer the values for the product of the density and specific heat were incremented 50% below and above the baseline value, and simulations produced temperatures within 0.098 ° C of the baseline value, again showing less sensitivity compared to soil parameters.
- *Heat transfer coefficient*. The heat transfer coefficient is the most uncertain parameter in the model, and it is often difficult to determine in all heat transfer models. To examine its sensitivity, values were taken over a full range, between 5 and 30 J/(cm^2 h °C). Temperature profiles differed from the baseline profile by at most 1.1425 °C, which occurred using the smallest value (5).

In summary, from the nest temperature model calculations we find the most sensitivity to changes in the thermal conductivity of the soil and the heat transfer coefficient. This conclusion may be expected because these two parameters have the greatest impact on the rate at which the heat is transferred through the soil to the nest. Although one may expect that the model is highly sensitive to the air-to-egg ratio of thermal conductivity (because of the very low thermal conductivity of air), the model shows only a maximum change of 0.28 ° C from the baseline. Therefore, we expect that models of nest temperatures in loamy soil, shaded areas, or subject to moisture events (which would affect conductivities) would give different population results.

Next we examine parameter sensitivity in the two-sex population model. Recall that the matrix is not a simple Leslie matrix and that the egg population equation is nonlinear with a 2-year recurrence relation; therefore, the population growth rate is not known a priori and a simple sensitivity or elasticity calculation is not possible. To examine the sensitivity of the parameters, we adjust each parameter individually, calculate the average year-to-year growth rate, and then compare to the baseline run. Baseline values are shown in Table 6, and we adjust each parameter within biologically measured values (Table 7).

- *Egg survivorship and hatchling graduation*. We adjust both the annual egg survivorship s_1 and hatchling graduation rates g_1 between 0.06 and 0.6, incrementing by 0.06. The computed population growth rates for egg survivorship and for hatchling graduation were in the ranges 0.92–1.05 and 0.92–1.05, respectively.
- *Survivorship and graduation rates for 2–3 year-olds*. The annual survivorship and graduation rates in the 2–3 year age class were examined in the interval 0.46–0.82, incrementing by 0.04. We adjusted for the 2-year time period as described earlier. The population growth rates were computed in the ranges 0.99–1.01 and 0.98–1.04, respectively.
- *Survivorship and graduation sensitivity for 4–5 and 6–7 year-olds*. The annual survivorship and graduation rates for both the 4–5 and 6–7 years age classes were examined within an interval 0.76–0.92, incrementing by 0.04, again adjusting for the 2-year time period as described earlier. Growth rates and survivorships and graduation for 4–5 years old were computed in the ranges 1.0–1.01 and 1.01–1.03, respectively. For 6–7 years old, the two ranges were 1.00–1.01 and 1.01–1.03, respectively.
- *8+ year-old survivorship sensitivity*. The annual survivorship rates for the 8+ year age classes were varied within the interval 0.76–0.96, incrementing by 0.04. Population growth rates increased from 0.94 to 1.07.
- *Probability of using current year's sperm*. We adjusted the probability of using the current year's sperm from 10% and 100%, incrementing by 10%. Several questions concerning sperm storage remain unanswered because there is little information or data concerning sperm storage. We do not know if sperm becomes less viable over time, or if the use of stored sperm is greater if the population is male-limited. The growth rates vary from 1.000 to 1.002.
- *Total eggs laid per female*. Sensitivity of the total eggs laid per female per year was changed from 6 to 24 eggs, giving growth rates between 0.95 and 1.05.
- *Number of females mated with, per male*. We varied the average number of females mated per male between 1.2 and 3, incrementing by 0.2. Females range between 39 and 414, with 117 and 1270 for eggs. Growth rates increased from 0.995 and 1.001.
- *Proportion of male eggs*. Finally, we look at the proportion of male eggs in the range of 20–80%, incrementing by 10%. Growth rates decreased from 1.01 to 0.97. In this case, as the proportion of male eggs increases, the male population actually decreases because the total number of eggs depends upon the number of females as well as the number of males. The fewer females there are to lay eggs, the fewer males there will be in the long term.

Table 6
Parameter values in the two-sex model baseline run.

Parameter	Value
s_1 and g_1	0.33
s_2	0.375
g_2	0.225
s_3 and s_4	0.4118
g_3 and g_4	0.2882
s_5	0.9
p	.5
q	.7
k	14
h	1.7

Table 7
Biologically measured values for each two-sex model parameter.

Parameter	Tinkle et al. (1981)	Mitchell (1988)	Wilbur (1975a,b)
s_1 and g_1	0.67	0.19	0.08
s_2 and g_2	0.76	0.46	0.82
s_3, s_4, g_3 and g_4	0.76	0.94	0.82
s_5	0.76	0.96	0.82

In summary, in the two-sex population model the parameters most sensitive to change are the total eggs laid k, adult survivorship s_5, egg survivorship s_1, and hatchling graduation rate. We also observe that in separate analyses for each set of data (Mitchell, 1988; Tinkle et al., 1981; Wilbur, 1975a), egg survivorship and hatchling graduation rates seem to strongly influence the survival of the population; those are the only rates that differ significantly among the different data sets.

5.2. Summary and future directions

Several problems suggest themselves for further investigations:

1. *Variable thermal conductivity with soil moisture*. In the model the effects of variable soil moisture were not included, nor were

rain events. The moisture content of the soil can significantly change the thermal conductivity of the soil (Buonanno et al., 1995) as well as the development time of the eggs (Ackerman et al., 1985a). Thus, the effects of moisture may play a significant role in the population dynamics.

2. *Variable sperm storage*. As noted, several questions concerning sperm storage remain unanswered because there is little information regarding sperm storage. We do not know, for example, if the use of stored sperm is greater if the population is male-limited. We tested this hypothesis crudely by assuming that the proportion of stored sperm usage is large when the male population is small by adjusting the two-sex model so that the proportion of sperm used from the current year is a function of the male population. That is,

$$q(m_n) = \frac{1}{1 + e^{-10((m/200)-.5)}},$$

where m_n is the number of males in year n. Again, because there is no data available, we chose a function that satisfies two criteria: first, it is an increasing function with range [0, 1], and second, it gives an output of approximately 0.7 at the baseline steady state. In this scenario, to cause a population to crash, we require extreme cases. The proportion of males in the starting population must be less than 30%, and the percentage of males from each clutch must be less than 20%. In the case where the beginning male-to-female ratio is 30:70 and the percentage of males from each clutch is 10%, the average growth rate of the male population is 0.96665 and the average growth rate of the female population is 0.98018. We also examined the effect of no sperm storage. Using the same starting ratios as above (male to female ratio of 30:70 and the percentage of males from each clutch being 10%), the average growth rate of the male population is 0.96333 and the female average growth rate is 0.97687. Thus, the computational model supports the hypothesis that there is an adaptive advantage to sperm storage. In these test simulations we ignored the survivorship of the eggs as accounting for the possibility of less viability in the older sperm. More experimental work is needed in this area to provide more accurate modeling of population dynamics.
3. *Variable absorption of solar radiation*. We assumed that the nest was under a smooth flat surface and the soil absorbed 80% of the solar radiation. We could examine perhaps more realistic cases by assuming that the ground that the soil has different reflective properties, or the nest is shaded. Either of these cases would change the absorption coefficient.
4. *Nest geometry, metabolic heat and clutch size*. In our model the soil inside and outside the nest had the same porosity and that the heat traveling horizontally between the nest and the surrounding soil does not affect the temperature of the nest. The geometry of the nest could be changed to a bounded cylinder with flux boundary conditions given on the surface. The calculation of heat flow in this case, three dimensions and time, would be computationally intensive.
5. *Metabolic heat*. If we take into account the metabolic heat generated by the eggs, which is a source term in the diffusion equation, the temperature inside the nest temperature could be strongly affected. As noted earlier, the nest temperature in this case is more likely to occur when the clutch size is larger. Also, we could consider that the sex of the turtle eggs depends not only on egg depth, but also upon the location within the nest; eggs near the center may be warmer than those on the outer edges.
6. *Different birth function*. We chose a birth function given by a harmonic mean. Equally, we could investigate the affects on population growth by using a different birth function.
7. *Female choice in nest site and nesting time*. We assumed female turtles do not consider the sex of her offspring when choosing a nest site or the mean date of first nest. It may be that shifts in the average temperature may lead to females choosing an earlier or later date for their first nest, or they may choose different nesting sites to compensate for a thermal shift, and thus maintain the current nest temperature conditions (Valenzuela and Lance, 2004). For example, models of alligator populations include nest site location (e.g., see Murray, 2002).

In summary, we showed how to formulate a detailed, complete model of TSD with the following elements: (1) stochastic temperature and solar radiation inputs, (2) a heat transfer model using the diffusion equation to obtain nest temperatures with different soil and egg layer conductivities, (3) a degree-day model to determine the sex of the nest with a temperature-dependent incubation period, and, (4) a two-sex, stage-based population model that includes male and female contributions to egg numbers, female sperm storage, and a polyandrous female population. Because of the model's flexibility, it can also be of great benefit to other researchers in the field who want to examine the effects of different temperatures and their variations on other species with TSD, e.g., crocodilians, as well as other turtle species. As we suggested, the temperature and conductivity are important inputs in the model, and they can be adapted to specialized environmental conditions, including temperature levels, nest location, soil type, and rain events. The TSD model easily accommodates different temperature ranges that apply to other species during their egg incubation period. The model also offers the opportunity to study density effects, for example, the dependence of the mating function on the ratio of males to females and each's contribution to the sex of the hatchlings. Other modifications of the two-sex population model are possible as well, in order to fit specific life history traits. The model is a beginning step in understanding the long term high fitness shown by many reptile species with TSD.

Acknowledgments

We are grateful to Professor Brigitte Tenhumberg (Biological Sciences and Mathematics) at the University of Nebraska Lincoln (UNL) for her insights and contributions regarding the modeling effort, to Professor Thomas Shores (Mathematics, UNL) for consultations on the numerical algorithms and the inverse problem, to Professor Larkin Powell (School of Natural Resources, UNL) for initiating and directing the experimental program on *C. picta* at Cedar Point Biological Station, and to Professor Nicole Valenzuela for early discussions on TSD in turtle populations. The research originated in the NSF sponsored RUTE program (Research for Undergraduates in Theoretical Ecology) at UNL, mentored by L. Powell and J.D. Logan, and directed by Professor Glenn Ledder (Mathematics, UNL), principal investigator on the RUTE grant; we greatly appreciate his strong support for the research project. Professor Bo Deng (Mathematics, UNL) read a draft of the paper, and we thank him for his input. A Matlab code that implements the model can be requested from the author A. Parrott (parrotta@uwosh.edu).

References

Ackerman, R., Dmi'el, R., Ar, A., 1985a. Energy and water vapor exchange by parchment-shelled reptile eggs. Physiological Zoology 58 (1), 129–137.
Ackerman, R., Dmi'el, R., Ar, A., 1985b. Water and heat exchange between parchment-shelled reptile eggs and their surroundings. Copeia (3), 703–711.
Anon., 2010. Earth Temperature and Site Geology. Virginia Department of Mines Minerals and Energy, Available at: http://www.geo4va.vt.edu/A1/A1.htm was accessed July 2007.
Bartlett, R.D., Bartlett, P.P., 2006. Guide and Reference to the Crocodilians, Turtles, and Lizards of Eastern and Central North America (North of Mexico). University Press of Florida, Gainesville, FL.

Bernstein, L., et al., 2007. Climate change 2007: synthesis report summary for policymakers. Technical report, Intergovernmental Panel on Climate Change.
Bull, J., 1985. Sex ratio and nest temperature in turtles: comparing field and laboratory data. Ecology 66 (4), 1115–1122.
Bull, J., Vogt, R., McCoy, C., 1982. Sex determining temperatures in turtles: a geographic comparison. Evolution 36 (2), 326–332.
Buonanno, G., Carotenuto, A., Dell'Isola, M., Villacci, D., 1995. Effect of radiative and convective heat transfer on thermal transients in power cables. IEE Proceedings-Generation, Transmission and Distribution 142 (4), 436–444.
Cagle, F., 1954. Observations on the life cycles of painted turtles (genus *Chryesmys*). American Midland Naturalist 52 (1), 225–235.
Cagle, K., Packard, G., Miller, K., Packard, M., 1993. Effects of the microclimate in natural nests on development of embryonic painted turtles, *Chrysemys picta*. Functional Ecology 7, 653–660.
Case, T.J., 2000. An Illustrated Guide to Theoretical Ecology. Oxford University Press, New York.
Caswell, H., 2001. Matrix Population Models, second edition. Sinauer Associates Inc., Sunderland, MA.
Chevalier, J., Godfrey, M., Girondot, M., 1999. Significant difference of temperature-dependent sex determination between French guiana (Atlantic) and playa grande (costa-rica, pacific) leatherbacks (*Dermochelys coriacea*). Annales des Sciences Naturelles 20 (4), 147–152.
Crouse, D., Crowder, L., Caswell, H., 1987. A stage-based population model for loggerhead sea turtles and implications for conservation. Ecology 68 (5), 1412–1423.
Demuth, J., 2001. The effects of constant and fluctuating incubation temperature on sex determination, growth, and performance in the tortois *Gopherus polyphemus*. Canadian Journal of Zoology 79, 1609–1620.
Du, W., Ji, X., 2003. The effects of incubation thermal environments on size, locomotor performance and early growth of hatchling soft-shelled turtles, *Pelodiscus sinensis*. Journal of Thermal Biology 28, 279–286.
Ellner, S.P., Guckenheimer, J., 2006. Dynamic Models in Biology. Princeton University Press, Princeton, NJ.
Engel, C., Åberg, P., Gaggiotti, O., Destombe, C., Valero, M., 2001. Population dynamics and stage structure in a haploiddiploid red seaweed, *Gracilaria gracilis*. Journal of Ecology 89, 436–450.
Ernst, C., Barbour, R., Lovich, J., 1994. Turtles of the United States and Canada. Smithsonian Institution Press, Washington.
Georges, A., 1989. Female turtles from hot nests: is it duration of incubation or proportion of development at high temperatures that matters? Oecologia 81, 323–328.
Georges, A., 1992. Thermal characteristics and sex determination in field nests of the pig-nosed turtle, *Carettochelys insculpta* (chelonia: Carettochelydidae) from northern Australia. Australian Journal of Zoology 40 (5), 511–521.
Georges, A., Beggs, K., Young, J., Doody, J., 2005. Modelling development of reptile embryos under fluctuating temperature regimes. Physiological and Biochemical Zoology 78 (1), 18–30.
Gibbons, J., 1968. Population structure and survivorship in the painted turtle, *Chrysemys picta*. Copeia (2), 260–268.
Gutzke, W., Packard, G., Packard, M., Boardman, T., 1987. Influence of the hydric and thermal environments on eggs and hatchlings of painted turtles (*Chrysemys picta*). Herpetologica 43 (4), 393–404.
Gutzke, W., Paukstis, G., 1984. A low threshold temperature for sexual differentiation in the painted turtle, *Chrysemys picta*. Copeia (2), 546–547.
Heppell, S., 1998. Application of life-history theory and population model analysis to turtle conservation. Copeia (2), 367–375.
Iverson, J., Simith, G., 1993. Reproductive ecology of the painted turtle (*Chrysemys picta*) in the nebraska sandhills and across its range. Copeia (1), 1–21.
Janzen, F., 1994. Climate change and temperature-dependent sex determination in reptiles. Proceedings of the National Academy of Sciences of the United States of America 91 (16), 7487–7490.
Janzen, F., Morjan, C., 2002. Egg size, incubation temperature, and posthatching growth in painted turtles (*Chrysemys picta*). Journal of Herpetology 36 (2), 308–311.
Janzen, J., Phillips, P., 2006. Exploring the evolution of environmental sex determination, especially in reptiles. Journal of Evolutionary Biology 19 (6), 1775–1784.
Lindström, Kokko, H., 1998. Sexual reproduction and population dynamics: the role of polygyny and demographic sex differences. Proceedings Royal Society of London, Biological Sciences 265 (1395), 483–488.
Logan, J.D., 1987. Applied Mathematics, A Contemporary Approach. John Wiley & Sons, New York.
Logan, J.D., Wolesensky, W., 2007. Accounting for temperature in predator functional responses. Natural Resource Modeling 20 (4), 549–574.
Logan, J.D., Wolesensky, W., Joern, A., 2006. Temperature-dependent phenology and predation in arthropod systems. Ecological Modelling 196, 471–482.
Maynard Smith, J., 1974. Models in Ecology. Cambridge University Press, Cambridge, UK.
Mitchell, J., 1988. Population ecology and life histories of the freshwater turtles *Chrysemys picta* and Sternotherus odoratus in an urban lake. Herpetological Monographs 2, 40–61.
Murray, J.D., 2002. Mathematical Biology I: An Introduction. Springer-Verlag, New York.
Natural Resources Conservation Service, Soil Climate Analysis Network (SCAN). Available at: http://www.wcc.nrcs.usda.gov/scan/.
Pearse, D., Avise, J., 2001. Turtle mating systems: behavior, sperm storage, and genetic paternity. The Journal of Heredity 92 (2), 206–211.
Pearse, D., Janzen, F., Avise, J., 2001. Genetic markers substantiate long-term storage and utilization of sperm by female painted turtles. Heredity 86, 378–384.
Pearse, D., Janzen, F., Avise, J., 2002. Multiple paternity, sperm storage, and reproductive success of female and male painted turtles (*Chrysemys picta*) in nature. Behavioral Ecology and Sociobiology 51 (2), 164–171.
Radiation, N.A.S., 1994. Average Monthly Minimum and Maximum Solar Radiation Tables. Available at: http://rredc.nrel.gov/solar/pubs/redbook/PDFs/NE.PDF.
Ranta, E., Kaitala, V., Lindstrom, J., 1999. Sex in space: population dynamic consequences. Proceedings Royal Society of London, Biological Sciences 266 (1424), 1155–1160.
Ranta, E., Kaitala, V., 1999. Punishment of polygyny. Proceedings Royal Society of London, Biological Sciences 2266 (1435), 2337–2341.
Rimkus, T., Hruska, N., Ackerman, R., 2002. Separating the effects of vapor pressure and heat exchange on water exchange by snapping turtle (*Chelydra serpentina*) eggs. Copeia (3), 706–715.
Rowe, J., Coval, K., Campbell, K., 2003. Reproductive characteristics of female midland painted turtles (*Chrysemys picta marginata*) from a population on beaver island, Michigan. Copeia (2), 326–336.
Schwarzkopf, L., Brooks, B., 1987. Nest-site selection and offspring sex ratio in painted turtles, *Chrysemys picta*. Copeia (1), 53–61.
Schwarzkpf, L., Brooks, R., 1985. Sex determination in northern painted turtles: effect of incubation at constant and fluctuating temperatures. Canadian Journal of Zoology 63, 2543–2547.
Shine, R., Harlow, P., 1996. Maternal manipulation of offspring phenotypes via nest-site selection in an oviparous lizard. Ecology 77 (6), 1808–1817.
Sundelöf, A., Åberg, P., 2006. Birth functions in stage structured two-sex models. Ecological Modeling 193, 787–795.
Tinkle, D., Congdon, J., Rosen, P., 1981. Nesting frequency and success: implications for the demography of painted turtles. Ecology 62 (6), 1426–1432.
Valenzuela, N., Lance, V.A. (Eds.), 2004. Temperature-Dependent Sex Determination in Vertebrates. Simthsonian Books, Washington.
Warner, D., Shine, R., 2008. The adaptive significance of temperature-dependent sex determination in a reptile. Nature 451 (31), 566–569.
Wilbur, H., 1975a. The evolutionary and mathematical demography of the turtle *Chrysemys picta*. Ecology 56, 64–77.
Wilbur, H., 1975b. A growth model for the turtle *Chrysemys picta*. Copeia (2), 337–343.
Woodward, D., Murray, J., 1993. On the effect of temperature-dependent sex determination on sex ratio and surviorship in crocodilians. Proceedings Royal Society of London, Biological Sciences 252 (1334), 149–155.
Yntema, C., 1968. A series of stages in the embryonic development of Chelydra serpentina. Journal of Morphology 125 (2), 219–252.